

QUANTUM OPTICS

PACS numbers: 42.50.Wk; 37.10.Vz
DOI: 10.1070/QE2014v044n10ABEH015377

Spectral anomalies of the effect of light-induced drift of caesium atoms caused by the velocity dependence of transport collision frequencies

A.I. Parkhomenko, A.M. Shalagin

Abstract. **The spectral features of the light-induced drift (LID) velocity of caesium atoms in inert buffer gases are studied theoretically. A strong temperature dependence of the spectral LID line shape of Cs atoms in Ar or Kr atmosphere in the vicinity of $T \sim 1000$ K is predicted. It is shown that the anomalous LID of Cs atoms in binary buffer mixtures of two different inert gases can be observed at virtually any (including ambient) temperature, depending on the content of the components in these mixtures. The results obtained make it possible to precisely test the interatomic interaction potentials in the experiments on the anomalous LID.**

Keywords: *light-induced drift, optical excitation, collisions, Doppler effect, buffer gas, kinetic equation.*

1. Introduction

The light-induced drift (LID), predicted theoretically [1] and first experimentally observed [2] in 1979, refers to a number of the most powerful effects of radiation on the translational motion of particles. The essence of the effect consists in the appearance of a directional macroscopic flow of particles that absorb radiation and are in a mixture with buffer particles. Recall the nature of the phenomenon. Due to the Doppler effect, radiation affects selectively the absorbing particle velocities, i.e., produces effective copropagating 'bundles' of particles in the excited and ground states. In a buffer gas atmosphere these bundles experience resistance due to the difference between the transport collision frequencies of excited and unexcited particles. As a result, the gas of the absorbing particles as a whole acquires a directional movement, and the particles can drift both in the direction of the luminous flux and in the opposite direction.

Theoretical and experimental studies have shown that the LID phenomenon is universal in the sense that it is implemented under typical experimental conditions and inherent in a wide class of objects: atoms, molecules, ions and conduction electrons in solids. To date, the LID effect has been experimentally observed for nearly two dozens of different objects – atoms (Li, Na, K, Rb, Ne, Ba) in various buffer gases, molecules (CH_3F, CH_3Br, C_2H_4, NH_3, SF_6, CH_3OH, H_2O, HF) in different buffer gases and electrons in the InSb semiconductor (see, for example, [3–9] and references therein).

Theoretically, under laser excitation the drift velocity caused by the LID effect can reach thermal velocity [10]. It has been experimentally shown that the atoms under the influence of the LID can drift at a velocity of 50 m s^{-1} [11].

One of the most important LID characteristics is the dependence of the drift velocity on the radiation frequency (LID line shape). The line shape of the LID observed in experiments has been historically used to distinguish between the 'normal' LID effect and the 'anomalous' one.

The normal LID effect is well described by the LID theory, which does not take into account the dependence of the resonant particles of transport collision frequencies on the velocity v. The drift velocity in the case of the normal LID is proportional to the relative difference $(\nu_e^{tr} - \nu_g^{tr})/\nu_g^{tr}$ between the average transport frequencies of collisions of resonant particles in the excited (e) and ground (g) states with the buffer particles. The average transport frequency ν_k^{tr} is related by a simple formula with the diffusion coefficient D_k of the particles in the state $k = e, g$ [3]: $\nu_k^{tr} = v_T^2/(2D_k)$, where v_T is the most probable velocity of the absorbing particles. Under the normal LID the dependence of the drift velocity on the radiation frequency has a simpler form. In particular, when excited by the particles on an isolated transition (two-level particles), this theory gives a characteristic dispersion-like (tilde-like) frequency dependence of the drift velocity with a zero at the zero detuning of the radiation frequency. Since the discovery of the LID effect (1979) and until 1992, all the experimental results of its investigation were in good agreement with this theory [3–7].

In the case of the anomalous LID effect, which was experimentally discovered in 1992 [12], there is a sharp deviation of the frequency dependence of the drift velocity from that predicted by the theory of the normal LID. By now, the anomalous LID has been studied in a significant number of experimental (the anomalous LID was observed for C_2H_4, HF and CH_3F molecules in various buffer gases [8, 9, 12–17], for potassium atoms in a buffer mixture of neon with other inert gases [18]) and theoretical [8, 15, 17, 19–26] papers. It was found that the anomalous LID is caused by the dependence of the transport collision frequencies on the velocity v of the resonant particles, wherein the anomality can arise only when the difference of the transport collision frequency $\Delta\nu(v) \equiv \nu_e(v) - \nu_g(v)$ of the particles at the combining (affected by radiation) levels e and g changes its sign as a function of v.

Because the transport collision frequencies $\nu_g(v)$ and $\nu_e(v)$ are entirely determined by the interaction potentials of the resonant and buffer particles, the line shape of the anomalous LID is very sensitive to the differences in the interaction

A.I. Parkhomenko Institute of Automation and Electrometry, Siberian Branch, Russian Academy of Sciences, prosp. Akad. Koptyuga 1, 630090 Novosibirsk, Russia; e-mail: par@iae.nsk.su;
A.M. Shalagin Institute of Automation and Electrometry, Siberian Branch, Russian Academy of Sciences, prosp. Akad. Koptyuga 1, 630090 Novosibirsk, Russia; Novosibirsk State University, ul. Pirogova 2, 630090 Novosibirsk, Russia; e-mail: shalagin@iae.nsk.su

Received 27 December 2013; revision received 13 February 2014
Kvantovaya Elektronika **44** (10) 928–938 (2014)
Translated by I.A. Ulitkin

potentials of the resonant atoms in the ground and excited states with the buffer particles. This allows for high-precision experimental testing of the LID of interatomic interaction potentials used to calculate the spectral shape of the anomalous LID signal, and, therefore, the possibility of a relatively simple experimental testing of the accuracy of various theoretical methods for calculating the interaction potentials.

In this paper, by using the known (calculated *ab initio*) interatomic Pascale and Vandeplanque interaction potentials [27], we have theoretically predicted and calculated the anomalous LID of caesium atoms in a single-component inert buffer gas or in different binary buffer mixtures of inert gases. We have determined the medium parameters (temperature, fractions of the components in the binary buffer mixture) at which one would expect the occurrence of the anomalous LID of Cs atoms. It has been found that the anomalous LID of Cs atoms in the binary buffer mixture of inert gases can be observed at virtually any (including at ambient) temperature, depending on the content of the buffer gas in the mixture. The calculations of the anomalous LID of Cs atoms provide experimenters with a selection of objects for tests in LID experiments on interatomic interaction potentials used to calculate the spectral line shape of the anomalous LID.

2. Initial equations and their solution

To calculate the LID velocity of alkali metal atoms, one should take into account the hyperfine structure (HFS) of the levels affected by radiation. One also should keep in mind the following fact. It is known that if the total orbital angular momentum of the electrons in the ground state is zero (S-state), the hyperfine sublevels can be extremely long-lived: collisions with nonmagnetic buffer gas particles virtually do not lead to mixing of the populations of these sublevels. For example, for the alkali metal atoms residing in the atmosphere of inert buffer gases, the cross sections of collisional transitions between the hyperfine structure components of the ground state are very small, i.e., by 6 to 10 orders of magnitude smaller than the gas-kinetic cross sections [28]. Due to this, the alkali metal atoms exhibit a highly pronounced effect of the so-called optical pumping (see, for example, [29]). The essence of the effect is that even weak optical radiation that is resonant with the transition to the nearest excited electronic state of the atoms can create a strong and long-lived nonequilibrium distribution of the population over the HFS sublevels of the ground state. In particular, this radiation can pump almost all the atoms (which effectively participate in the interaction) to one of the HFS components. In fact, the greater the hyperfine splitting in comparison with the Doppler linewidth, the more pronounced the pumping from one hyperfine component of the ground state to the other. Of alkali atoms we should particularly single out the Cs atoms, where the hyperfine splitting is equal to 40 Doppler widths.

Optical pumping, so essential in the case of large hyperfine splitting of the electronic ground state of the caesium atoms, significantly decreases the LID velocity. The strong influence of optical pumping can be drastically reduced by exciting caesium atoms at two different frequencies chosen such that each radiation affects different hyperfine sublevels of the ground state. We assume that one radiation is monochromatic, and the other is broadband with a spectral width larger than the Doppler linewidth. Monochromatic radiation affects selectively the absorbing particle velocity and therefore provides the occurrence of the LID effect. Broadband radiation that interacts nonselectively with the velocity of the atoms does not lead to the emergence of the LID effect, but causes its manifold increase due to the fact that it radically reduces the optical pumping. At the same time one can expect that the drift velocity will be of the same order of magnitude as that for the two-level particles. In view of this fact, we will assume below in the calculation of the LID velocity of alkali metal atoms that the atoms are excited by two-frequency radiation.

Consider a gas of the absorbing particles with a HFS of the ground and excited states; the gas being mixed with a buffer gas. Let the subscript $i = 1, 2, 3, 4$ denote the number of the HFS sublevels of the excited state e, and the subscript $j = \mathrm{n}, \mathrm{m}$ – the HFS sublevels of the lower (ground) state g. The degeneracy of the levels i, j in the directions of the magnetic moment will be taken into account by the introduction of the statistical weights g_i, g_j. We will neglect the collisions between the absorbing particles by assuming the concentration of the buffer gas N_b to be much greater than that of the absorbing gas N.

The interaction of the absorbing particles of the gas with resonance radiation in stationary and spatially homogeneous conditions is described by the equations for the velocity distributions of the populations $\rho_i(\boldsymbol{v})$ and $\rho_j(\boldsymbol{v})$ of the HFS sublevels i and j:

$$\begin{aligned} &S_i(\boldsymbol{v}) + N\sum_j P_{ji}(\boldsymbol{v}) - \Gamma_\mathrm{e}\rho_i(\boldsymbol{v}) = 0, \\ &S_j(\boldsymbol{v}) - N\sum_i P_{ji}(\boldsymbol{v}) + \sum_i \Gamma_{ij}\rho_i(\boldsymbol{v}) = 0, \end{aligned} \tag{1}$$

where

$$N = N_\mathrm{e} + N_\mathrm{g}; \quad N_\mathrm{e} = \sum_i N_i; \quad N_\mathrm{g} = \sum_j N_j;$$

$$N_i = \int \rho_i(\boldsymbol{v})\,\mathrm{d}\boldsymbol{v}; \quad N_j = \int \rho_j(\boldsymbol{v})\,\mathrm{d}\boldsymbol{v}; \tag{2}$$

N_i and N_j are the partial (over the HFS sublevels) concentrations of the absorbing particles; N_e and N_g are the concentrations of the absorbing particles in the excited and ground states, respectively; Γ_{ij} is the rate of spontaneous decay of the excited state i via $i \to j$; Γ_e is the total rate of spontaneous decay of the excited level e; $S_i(\boldsymbol{v})$ and $S_j(\boldsymbol{v})$ are the collision integrals; and $P_{ji}(\boldsymbol{v})$ is the probability of absorption per unit time on the $j \to i$ transition per one absorbing atom with a predetermined velocity v.

The rate Γ_{ij} of the radiative transition between the HFS sublevels of the excited, $|i\rangle = |J_\mathrm{e}, I, F_i\rangle$, and ground, $|j\rangle = |J_\mathrm{g}, I, F_j\rangle$, states is given by the expression [30]:

$$\Gamma_{ij} = \Gamma_\mathrm{e}(2J_\mathrm{e} + 1)(2F_j + 1)\begin{Bmatrix} J_\mathrm{e} & F_i & I \\ F_j & J_\mathrm{g} & 1 \end{Bmatrix}, \tag{3}$$

where

$$\begin{Bmatrix} a & b & c \\ d & e & f \end{Bmatrix}$$

is the $6j$-symbol [30, 31]; I is the nuclear spin of the atom; J_e and J_g are the total moments of the electron shell of the atom in the excited and ground states, respectively; and F_i, F_j are the total moments of the atom (with the nucleus) for the corresponding hyperfine components. By using the well-

known formulas for 6*j*-symbols [30, 31] it is easy to see that the spontaneous decay rates Γ_{ij} obey the relations

$$\sum_j \Gamma_{ij} = \Gamma_e, \quad \sum_i w_i \Gamma_{ij} = w_j \Gamma_e, \tag{4}$$

where $w_i = g_i / \sum_{i'} g_{i'}$ and $w_j = g_j / \sum_{j'} g_{j'}$ are the relative statistical weights of the sublevels i and j ($g_i = 2F_i + 1$, $g_j = 2F_j + 1$). The first relation in (4) demonstrates the well-known fact [30] that the total rate Γ_e of spontaneous decay of the excited hyperfine sublevel i is the same for all hyperfine sublevels i of the excited state e. The essence of the second relation in (4) is that in the case of the equilibrium distribution of the particles in the hyperfine components of the excited state, the spontaneous decay also leads to the equilibrium population of the HFS sublevels of the lower state.

Let us find the radiation absorption probability $P_{ji}(\boldsymbol{v})$ in equations (1). For simplicity, we restrict our consideration to the condition of weak intensities of monochromatic and broadband radiations and assume that the fraction of the particles in the excited state e is small ($N_e \ll N$), and the velocity distribution of the populations of the hyperfine components $j = n, m$ in the ground state g is close to Maxwellian:

$$\rho_j(\boldsymbol{v}) = N_j W(\boldsymbol{v}), \tag{5}$$

where $W(\boldsymbol{v})$ is the Maxwellian distribution. Under these conditions, the radiation absorption probability $P_{ji}(\boldsymbol{v})$ in (1) is defined by the well-known expression:

$$\begin{aligned} P_{ji}(\boldsymbol{v}) &= B_{ji} \frac{N_j}{N} W(\boldsymbol{v}) [I_m Y_{ji}(\boldsymbol{v}) + I_b Y_{ji}^b(\boldsymbol{v})], \\ Y_{ji}(\boldsymbol{v}) &= \frac{1}{\pi} \frac{\Gamma(v)}{\Gamma^2(v) + (\omega - \omega_{ij} - \boldsymbol{kv})^2}, \\ Y_{ij}^b(\boldsymbol{v}) &= \frac{1}{\pi} \int_0^\infty \frac{\Gamma(v) F(\omega)}{\Gamma^2(v) + (\omega - \omega_{ij} - \boldsymbol{k}_b \boldsymbol{v})^2} \, d\omega, \\ \int_0^\infty F(\omega) \, d\omega &= 1, \quad B_{ji} = \frac{\lambda^2 \Gamma_e}{4\hbar\omega} \frac{g_i \Gamma_{ij}}{g_j \Gamma_e}, \end{aligned} \tag{6}$$

where ω, λ, $\boldsymbol{k}$ and I_m are the frequency, wavelength, wave vector and intensity of monochromatic radiation; $\boldsymbol{k}_b$ and I_b are the wave vector and intensity of broadband radiation; $F(\omega)$ is the line shape of broadband radiation; ω_{ij} is the resonant frequency of the $j \to i$ transition; B_{ji} is the second Einstein coefficient [30] (we assume that this coefficient is the same for monochromatic and broadband radiations because of the smallness of the hyperfine splitting frequency compared to the optical frequency); and $\Gamma(v)$ is the homogeneous half-width of the absorption line, which generally depends on the velocity and is the sum of the spontaneous, $\Gamma_e/2$, and collision, $\gamma(v)$, half-widths:

$$\Gamma(v) = \Gamma_e/2 + \gamma(v). \tag{7}$$

Formula (6) for the absorption probability $P_{ji}(\boldsymbol{v})$ includes N_j, i.e., the populations of the jth HFS sublevel of the ground state. The populations N_j can be found from equations (1) integrated over the velocities. For the velocity-averaged collision integrals we use the model expressions:

$$\begin{aligned} \int S_i(\boldsymbol{v}) \, d\boldsymbol{v} &= \bar{\nu}_e (w_i N_e - N_i), \\ \int S_j(\boldsymbol{v}) \, d\boldsymbol{v} &= \bar{\nu}_g [w_j (N_m + N_n) - N_j]. \end{aligned} \tag{8}$$

The frequencies $\bar{\nu}_e$ and $\bar{\nu}_g$ denote the frequencies of collisional mixing of the HFS components of the excited and ground states, respectively. It is assumed that each effective collision frequency, characterised by the frequency $\bar{\nu}_e$ ($\bar{\nu}_g$), leads to an equilibrium distribution of the populations of the HFS components of the e (g). Taking into account (8) and (6), the balance equations for the populations $N_{i,j}$ have the form

$$\begin{aligned} &\bar{\nu}_e (w_i N_e - N_i) + Q_{mi} N_m + Q_{ni} N_n - \Gamma_e N_i = 0, \\ &\bar{\nu}_g [w_j (N_m + N_n) - N_j] - \sum_i Q_{ji} N_j + \sum_i \Gamma_{ij} N_i = 0, \end{aligned} \tag{9}$$

where

$$Q_{ji} = B_{ji} \int [I_m Y_{ji}(\boldsymbol{v}) + I_b Y_{ji}^b(\boldsymbol{v})] W(\boldsymbol{v}) \, d\boldsymbol{v}. \tag{10}$$

Using the approximate normalisation condition $N_m + N_n \simeq N$ (here we have taken into account the approximation $N_e \ll N$) and relations (4), from equation (9) we obtain the expressions for the relative populations of the HFS sublevels of the ground state:

$$\begin{aligned} \frac{N_m}{N} &= \frac{w_m \bar{\nu}_g (\Gamma_e + \bar{\nu}_e) + \sum_i Q_{ni} (\Gamma_{im} + w_m \bar{\nu}_e)}{\bar{\nu}_g (\Gamma_e + \bar{\nu}_e) + \sum_i Q_{ni} (\Gamma_{im} + w_m \bar{\nu}_e) + \sum_i Q_{mi} (\Gamma_{in} + w_n \bar{\nu}_e)}, \\ \frac{N_n}{N} &= 1 - \frac{N_m}{N}, \end{aligned} \tag{11}$$

where the summation is performed over all allowed transitions $n, m \to i$. The population of the excited state is neglected.

Let us derive an expression for the drift velocity from the kinetic equations (1). Note that the hyperfine states are the result of interaction between the electrons of an atom with the angular momentum (spin) of the nucleus. The nuclear spin has little effect on the atomic electron shell, which determines the interaction potential in collisions and therefore the collision characteristics of the atoms. Consequently, the absorbing atoms at different sublevels 'inside' its HFS have almost identical interaction potentials in collisions with the buffer gas atoms. Thus, the collision characteristics of the atoms can differ only for thin components (e.g., $P_{1/2}$ and $P_{3/2}$) and for the ground state ($S_{1/2}$). This approximation allows us, by summing the equation in (1) with respect to i and j, to derive the equations:

$$\begin{aligned} &S_e(\boldsymbol{v}) + NP(\boldsymbol{v}) - \Gamma_e \rho_e(\boldsymbol{v}) = 0, \\ &S_g(\boldsymbol{v}) - NP(\boldsymbol{v}) + \Gamma_e \rho_e(\boldsymbol{v}) = 0, \end{aligned} \tag{12}$$

where $\rho_e(\boldsymbol{v}) = \sum_i \rho_i(\boldsymbol{v})$ [$\rho_g(\boldsymbol{v}) = \sum_j \rho_j(\boldsymbol{v})$] is the total population of the excited (ground) state;

$$\begin{aligned} P(\boldsymbol{v}) &= \sum_{i,j} P_{ji}(\boldsymbol{v}) \\ &= W(\boldsymbol{v}) \sum_j \frac{N_j}{N} \sum_i B_{ji} [I_m Y_{ji}(\boldsymbol{v}) + I_b Y_{ji}^b(\boldsymbol{v})] \end{aligned} \tag{13}$$

is the sum of the absorption probabilities (6) over all allowed transitions; $S_e(\boldsymbol{v}) = \sum_i S_i(\boldsymbol{v})$; and $S_g(\boldsymbol{v}) = \sum_j S_j(\boldsymbol{v})$. For the collision integrals in (12) we use the model of particle 'arrival' that is isotropic in velocities [25, 32]:

$$S_k(\boldsymbol{v}) = -\nu_k(v)\rho_k(\boldsymbol{v}) + S_k^{(2)}(v), \quad k = \mathrm{e}, \mathrm{g}, \tag{14}$$

where the 'arrival' term $S_k^{(2)}(v)$ is the function of the velocity modulus $v = |\boldsymbol{v}|$; and $\nu_k(v)$ is the transport collision frequency [23, 32]. The collision model (14) takes into account the velocity dependence of the collision frequency and at the same time allows one to obtain an analytical solution to the problem in question at any ratios of the masses of active and buffer particles.

The transport collision frequency $\nu_k(v)$ in (14) is related with the characteristics of the elementary scattering event by the expression [3]

$$\nu_k(v) = \frac{q}{v^3}\int_0^\infty u^2 \exp\left(-\frac{u^2+v^2}{\bar{v}_b^2}\right) F(uv)\sigma_k(u)\,\mathrm{d}u, \tag{15}$$

where

$$\begin{aligned} &F(uv) = \frac{2uv}{\bar{v}_b^2}\cosh\left(\frac{2uv}{\bar{v}_b^2}\right) - \sinh\left(\frac{2uv}{\bar{v}_b^2}\right);\\ &q = \frac{\mu}{M}\frac{N_b\bar{v}_b}{\sqrt{\pi}}; \quad \mu = \frac{MM_b}{M+M_b}; \quad \bar{v}_b = \sqrt{\frac{2k_BT}{M_b}}; \end{aligned} \tag{16}$$

N_b and M_b are the concentration and the mass of the buffer particles; M is the mass of the particles absorbing radiation; k_B is the Boltzmann constant; T is the temperature; u is the relative velocity of the resonant and buffer particles before the collision; $\sigma_k(u)$ is the transport scattering cross section of the absorbing particle in the k state by the buffer particle. The cross sections $\sigma_k(u)$ are calculated using the interaction potentials of the absorbing and buffer particles.

The LID velocity of the absorbing particles is given by

$$\boldsymbol{u}_L = \frac{1}{N}\int \boldsymbol{v}[\rho_e(\boldsymbol{v}) + \rho_g(\boldsymbol{v})]\,\mathrm{d}\boldsymbol{v}. \tag{17}$$

From the structure of equations (12) and expression (13), taking into account the specific form of the collision integral (14), it follows that the velocity distributions of the populations $\rho_e(\boldsymbol{v})$ and $\rho_g(\boldsymbol{v})$ represent the sum of the anisotropic parts $\delta\rho_e(\boldsymbol{v})$ and $\delta\rho_g(\boldsymbol{v})$ directly induced by radiation [the function $P(\boldsymbol{v})$] and the isotropic parts generated by the term of the 'arrival' of the collision integral (14). It is obvious that only the anisotropic parts of the velocity distribution of the populations contribute to the drift velocity (17). For these anisotropic parts from equations (12) with (14) taken into account, we obtain the expressions:

$$\begin{aligned} &\delta\rho_e(\boldsymbol{v}) = N\frac{P(\boldsymbol{v})}{\Gamma_e + \nu_e(v)},\\ &\delta\rho_g(\boldsymbol{v}) = -N\frac{\nu_e(v)P(\boldsymbol{v})}{\nu_g(v)[\Gamma_e + \nu_e(v)]}. \end{aligned} \tag{18}$$

When substituting formulas (18) into (17) for the drift velocity, we obtain the expression

$$\boldsymbol{u}_L = \int \frac{\nu_g(v) - \nu_e(v)}{\nu_g(v)[\Gamma_e + \nu_e(v)]}\,\boldsymbol{v}P(\boldsymbol{v})\,\mathrm{d}\boldsymbol{v}. \tag{19}$$

As noted in the Introduction, the anomalous LID can arise when the transport frequencies [$\nu_e(v)$ and $\nu_g(v)$] of collisions of the resonant particles in the excited and ground states with the buffer particles are close to each other. The cause for the anomalous LID emergence is the difference in dependences $\nu_e(v)$ and $\nu_g(v)$ and, as a consequence, the possibility of changing the sign of the difference in the transport collision frequencies, $\Delta\nu(v) \equiv \nu_e(v) - \nu_g(v)$. In this case, the absorbing particles with both a positive and a negative value of $\Delta\nu(v)$ contribute to the drift velocity $\boldsymbol{u}_L$. This can lead to a strong deviation of the LID line shape from that predicted by the theory of the normal LID effect, which does not take into account the velocity dependence of the transport collision frequencies.

If the frequencies $\nu_e(v)$ and $\nu_g(v)$ strongly differ from each other, the drift velocity $\boldsymbol{u}_L$ as a function of the radiation frequency corresponds to the normal LID and is well described by the LID theory with velocity-independent transport collision frequencies, i.e., by replacing in expression (19) the frequency $\nu_k(v)$ ($k = \mathrm{e}, \mathrm{g}$) by the average transport frequency

$$\begin{aligned} \nu_k^{\mathrm{tr}} &= \frac{2}{v_T^2}\int (\boldsymbol{nv})^2 W(\boldsymbol{v})\nu_k(v)\,\mathrm{d}\boldsymbol{v}\\ &= \frac{8}{3\sqrt{\pi}}\frac{\mu}{M}\frac{N_b}{u_T^5}\int_0^\infty u^5 \exp\left(-\frac{u^2}{u_T^2}\right)\sigma_k(u)\,\mathrm{d}u, \end{aligned} \tag{20}$$

where $v_T = (2k_BT/M)^{1/2}$ is the most probable velocity of the absorbing particles; $u_T = (2k_BT/\mu)^{1/2}$ is the most probable velocity of the relative motion of the absorbing and buffer particles; and $\boldsymbol{n}$ is the unit vector in the arbitrary direction. The average transport frequency ν_k^{tr} is related by a simple formula with the diffusion coefficient D_k of the particles in the k state [3, 33]:

$$\nu_k^{\mathrm{tr}} = \frac{v_T^2}{2D_k}. \tag{21}$$

Expression (19) for the drift velocity, which is a three-dimensional integral, can be greatly simplified by integrating the velocity $\boldsymbol{v}$ over the directions. As a result, we obtain the final expression for the drift velocity $\boldsymbol{u}_L$, which is given in the form

$$\boldsymbol{u}_L \equiv u_0\boldsymbol{u}(\Omega), \tag{22}$$

where we have introduced the velocity parameter u_0

$$u_0 = \frac{\lambda^4 I_m}{8\pi^{7/2}\hbar c}, \tag{23}$$

and the dimensionless velocity $\boldsymbol{u}(\Omega)$, which depends on the frequency detuning Ω of monochromatic radiation

$$\begin{aligned} \boldsymbol{u}(\Omega) = \int_0^\infty t\tau(t)\exp(-t^2)\sum_j\frac{N_j}{N}\sum_i\xi_{ji}\\ \times\left[\frac{\boldsymbol{k}}{k}f_{ij}(t) + \frac{\boldsymbol{k}_b}{k_b}\frac{I_b}{I_m}\int_0^\infty f_{ij}(t)F(\omega)\,\mathrm{d}\omega\right]\mathrm{d}t. \end{aligned} \tag{24}$$

Here we use the function of the dimensionless velocity $t = v/v_T$:

$$f_{ij}(t) = x_{ij}\psi_{ij}(t) + \frac{y(t)}{2}\ln\frac{y^2(t)+(t-x_{ij})^2}{y^2(t)+(t+x_{ij})^2},$$

$$\psi_{ij}(t) = \arctan\frac{t+x_{ij}}{y(t)} + \arctan\frac{t-x_{ij}}{y(t)},$$

$$\tau(t) = \frac{\nu_g(t)-\nu_e(t)}{\nu_g(t)}\frac{\Gamma_e}{\Gamma_e+\nu_e(t)}, \quad (25)$$

$$y(t) = \frac{\Gamma(t)}{kv_T}, \quad x_{ij} = \frac{\omega-\omega_{ij}}{kv_T}, \quad \xi_{ij} = \frac{g_i}{g_j}\frac{\Gamma_{ij}}{\Gamma_e}.$$

In expression (24), the relative populations of the HFS sublevels of the ground state N_j/N are found from formula (11) using the Q_{ji} quantities (10), which take the form

$$Q_{ji} = \frac{2B_{ji}}{\pi^{3/2}kv_T}\int_0^\infty t\exp(-t^2) \times\left[I_m\psi_{ij}(t) + I_b\int_0^\infty \psi_{ij}(t)F(\omega)\,d\omega\right]dt. \quad (26)$$

As the frequency detuning Ω of monochromatic radiation it is convenient to introduce in (24) the quantity

$$\Omega = \omega - \omega_0, \quad (27)$$

where ω_0 is the frequency between the 'middles' of the HFS of the excited and ground states.

Thus, the calculation of the drift velocity by the collision model (14) of the velocity-isotropic 'arrival' and by taking into account the dependence of the collision broadening on the velocity v of the resonant particles is reduced to the calculation of integrals (24) and (26).

When calculating the LID velocity of the atoms in the mixture of two different buffer gases, in formula (25) we must assume for $\tau(t)$ that

$$\nu_k(t) = \nu_{1k}(t) + \nu_{2k}(t), \quad (28)$$

where the subscripts 1 and 2 denote the sort of the buffer particles. Similarly, the total collision half-width of the absorption line $\gamma(t)$ is equal to the sum of half-widths $\gamma_1(t)$ and $\gamma_2(t)$, caused by the collision interaction of buffer particles of sorts 1 and 2.

It is appropriate to make a remark. In the initial equations describing the LID effect of alkali metal atoms, we neglected the effect of light pressure. This was due to the fact that under conditions typical for the occurrence of the LID, the effect of light pressure is several orders of magnitude weaker because the photon momentum is small as compared with the characteristic thermal momentum of the particle [3].

In order to compare the effects of the LID and light pressure, we present a formula for the velocity $\boldsymbol{u}_R$ of the drift caused by light pressure. For simplicity, we consider the case when the transport collision frequency $\nu_k(v)$ and the homogeneous half-width of the absorption line $\Gamma(v)$ are independent of the velocity v [$\nu_k(v) = \nu_k^{tr} = \text{const}$, $\Gamma(v) = \Gamma = \text{const}$]. Under these conditions, the drift velocity $\boldsymbol{u}_R$ is given by the expression (see, e.g., [3]):

$$\boldsymbol{u}_R = \frac{\hbar\boldsymbol{k}}{M}\frac{P_m}{\nu_g^{tr}} + \frac{\hbar\boldsymbol{k}_b}{M}\frac{P_b}{\nu_g^{tr}}, \quad (29)$$

where $\hbar\boldsymbol{k}/M$ and $\hbar\boldsymbol{k}_b/M$ are the recoil velocities during absorption of the photons of monochromatic and broadband radiations, respectively;

$$P_m = \sum_j\frac{N_j}{N}\sum_i Q_{ji}^m, \quad P_b = \sum_j\frac{N_j}{N}\sum_i Q_{ji}^b \quad (30)$$

are the velocity-integrated absorption probabilities of monochromatic (P_m) and broadband (P_b) radiations per unit of time; and Q_{ji}^m and Q_{ji}^b are, respectively, the first term (proportional to the intensity I_m of monochromatic radiation) and the second term (proportional to the intensity I_b of broadband radiation) in formula (26) for Q_{ji}. The sum $P_m + P_b$ gives a complete, velocity-integrated probability P of radiation absorption by a particle per unit of time:

$$P_m + P_b = P \equiv \int P(\boldsymbol{v})\,d\boldsymbol{v} = \sum_j\frac{N_j}{N}\sum_i Q_{ji}. \quad (31)$$

3. Anomalous LID of caesium atoms

The transport properties of Cs atoms in the excited states $6^2P_{1/2}$ and $6^2P_{3/2}$ are different in view of the fact that due to the large value of the Massey parameter, the collisional mixing of the fine structure components of caesium atoms is absent (see, for example, [34]). In this case, the $6^2P_{1/2}$ and $6^2P_{3/2}$ states are excited differently by the collisions. Therefore, the anomalous LID arises in a different manner for the cases of excitation of D_1 and D_2 transitions of caesium atoms.

Using formulas (15) and (22)–(26), we have numerically investigated the LID of caesium atoms in inert buffer gases. Figure 1 shows the energy level diagram of caesium atoms ^{133}Cs for the transitions $6^2S_{1/2}$–$6^2P_{1/2}$ (D_1 line) and $6^2S_{1/2}$–$6^2P_{3/2}$ (D_2 line). For caesium atoms, according to the NIST database [35], the spontaneous decay rates Γ_e of the excited levels

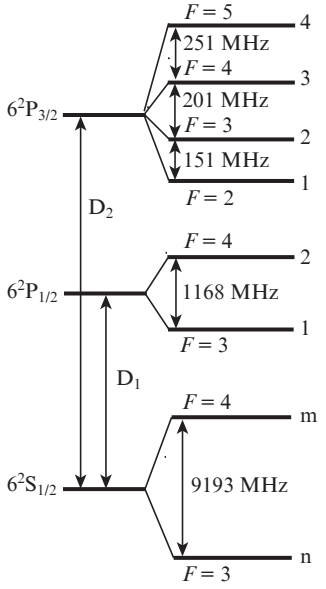

Figure 1. Energy level diagram of caesium atoms ^{133}Cs (nuclear spin, $I = 7/2$) involved in the $6^2S_{1/2}$–$6^2P_{1/2}$ (D_1 line, $\lambda = 894.3$ nm) and $6^2S_{1/2}$–$6^2P_{3/2}$ (D_2 line, $\lambda = 852.1$ nm) transitions:
F is the total angular momentum of the atom; n, m, 1, 2, 3, 4 are designations of the HFS sublevels used in text.

$6^2P_{1/2}$ and $6^2P_{3/2}$ are 2.86×10^7 and 3.28×10^7 s^{-1}, respectively; the wavelength of the D_1 line is λ = 894.3 nm; and the wavelength D_2 line is λ = 852.1 nm. The rates Γ_{ij} of the radiative transition between the magnetic HFS sublevels are calculated using formula (3).

It is usually assumed in the LID theory that the collision half-width of the absorption line $\gamma(v)$ is independent of the velocity v of the resonant particles [$\gamma(v) = \gamma$ = const]. In the case of the normal LID [when the difference in the transport collision frequencies $\Delta\nu(v)$ does not change its sign as a function of v], the effect of the dependence $\gamma(v)$ on the LID line shape is negligible and can be ignored. This effect is also negligible in the case of the anomalous LID if the Doppler width of the absorption line markedly exceeds its collision half-width (at $\gamma \ll kv_T$, kv_T is the Doppler width) [25, 36]. That is why in calculating the LID velocity in terms of Doppler broadening, we have neglected the dependence of the homogeneous half-width of the absorption line $\Gamma(v)$ of the velocity v and set $\Gamma(t) = \Gamma$ = const in formulas (25). The specific values of $\Gamma = \Gamma_e/2 + \gamma$ for different Cs–X systems (X is the inert gas atom) were determined according to [37] for the coefficients β of the collision broadening of the absorption line (in the case of D_1 and D_2 lines we, respectively, have β_{He} = 9.62 and 13.35 MHz Torr^{-1} for Cs–He; β_{Ne} = 5.01 and 5.20 MHz Torr^{-1} for Cs–Ne; β_{Ar} = 9.82 and 11.39 MHz Torr^{-1} for Cs–Ar; β_{Kr} = 9.92 and 5.40 MHz Torr^{-1} for Cs–Kr; and β_{Xe} = 10.70 and 28.77 MHz Torr^{-1} for Cs–Xe).

For alkali metal atoms in the atmosphere of inert buffer gases, the collision cross sections of the n → m and m → n transitions between the HFS components of the ground state are very small, i.e., by 6 to 10 orders of magnitude less than the gas-kinetic cross sections [28]. Therefore, we assume that the frequency of collisional mixing of the HFS components of the ground state is $\bar{\nu}_g = 0$. At the same time, the populations of the HFS components of the excited state are easily mixed in collisions [28]. In view of this fact, for the frequency $\bar{\nu}_e$ of collisional mixing of the HFS components of the excited state, we will use the same values as for the collision half-widths ($\bar{\nu}_e = \gamma$).

The transport collision frequencies $\nu_k(t) \equiv \nu_k(tv_T) \equiv \nu_k(v)$ for the Cs–X systems were calculated numerically by formula (15) using the transport cross sections $\sigma_k(u)$ from [22, 23] on the basis of the Pascale and Vandeplanque potential interaction [27].

A good criterion for determining the possibility of the anomalous LID occurrence in a single-component buffer gas is the sign-alternating temperature dependence of the difference between the averaged transport frequencies of collisions with the buffer particles (20) $\nu_e^{tr} - \nu_g^{tr}$ or, which is the same, the difference between the diffusion coefficients in the buffer gas $D_e - D_g$ of the resonant atoms in the excited and ground states. In the case of the binary buffer mixture the criterion for the occurrence of the anomalous LID are different signs of the difference $\nu_e^{tr} - \nu_g^{tr}$ for the resonant atoms in each of the two buffer gases. The anomalous LID should be expected to arise in a single-component buffer gas at such temperatures and such relative fractions of gases in the binary buffer mixture, for which the difference $\nu_e^{tr} - \nu_g^{tr}$ (or $D_e - D_g$) vanishes (under these conditions, the velocity dependence of the collision frequencies will become pronounced). The above criteria were used in [18, 22, 23, 25, 26] to find the objects that 'claim' to exhibit the anomalous LID.

Figures 2 and 3 shows the temperature dependence of the relative difference

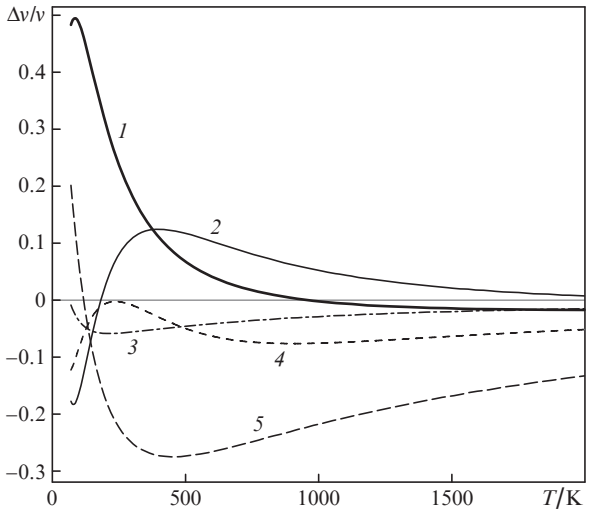

Figure 2. Temperature dependences of the relative difference $\Delta\nu/\nu \equiv (\nu_e^{tr} - \nu_g^{tr})/\nu_g^{tr}$ between the average transport frequencies of collisions of caesium atoms in the excited (e) and ground (g) states with the inert gas atoms upon excitation of the $6^2S_{1/2}$–$6^2P_{1/2}$ (D_1 line) transition of Cs atoms in the mixtures of (*1*) Cs–Ar, (*2*) Cs–Xe, (*3*) Cs–He, (*4*) Cs–Kr and (*5*) Cs–Ne.

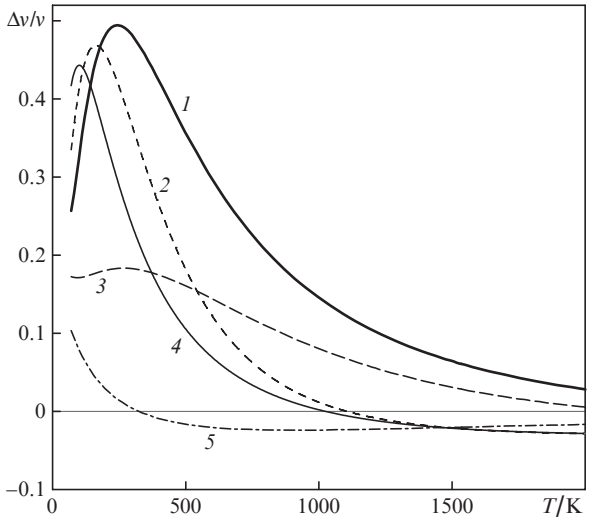

Figure 3. Same as in Fig. 2, but upon excitation of the $6^2S_{1/2}$–$6^2P_{3/2}$ (D_2 line) transition of Cs atoms in mixtures of (*1*) Cs–Xe, (*2*) Cs–Kr, (*3*) Cs–Ne, (*4*) Cs–Ar and (*5*) Cs–He.

$$\frac{\Delta\nu}{\nu} \equiv \frac{\nu_e^{tr} - \nu_g^{tr}}{\nu_g^{tr}} \tag{32}$$

of the average transport frequencies of collisions of caesium atoms in the excited and ground states with the inert gas atoms during the excitation of the $6^2S_{1/2}$–$6^2P_{1/2}$ (D_1 line) and $6^2S_{1/2}$–$6^2P_{3/2}$ (D_2 line) transitions of Cs atoms. For the factor $\Delta\nu/\nu$, to which the drift velocity of the normal LID is proportional, we have found a strong temperature dependence, up to a change of sign for some pairs of colliding particles.

In exciting the D_1 transition of Cs atoms in the Ar buffer gas, the factor $\Delta\nu/\nu$ vanishes at $T \approx 960$ K [curve (*1*) in Fig. 2]. Therefore, the anomalous LID should arise in the vicinity of $T \approx 960$ K. Analysis of Fig. 2 shows that the anomalous LID should also be expected to occur upon excitation of the D_1 transition of Cs atoms in mixtures of inert gases Ne–Ar,

Ne–Xe, He–Ar, He–Xe, Kr–Ar and Kr–Xe almost at any temperatures (depending on the choice of the buffer gas fraction in the binary buffer mixture).

In exciting the D_2 transition of Cs atoms in any of the buffer gases – Kr, Ar or He, the factor $\Delta v/v$ vanishes at temperatures $T \approx 1106$, ~1025 or ~325 K, respectively [curves (*2*, *4*, *5*) in Fig. 3]. Therefore, the anomalous LID of Cs atoms should arise in the specified buffer gases in the vicinity of these temperatures. It also follows from the analysis of Fig. 3 that upon excitation of the D_2 transition of Cs atoms, the anomalous LID should be expected to arise in the mixtures of inert gases He–Ne, He–Ar, He–Kr and He–Xe at $T > 325$ K (the temperature depends on the choice of the buffer gas fraction in the binary buffer mixture).

Figure 4 shows the dependences [calculated by formula (15)] of the relative difference

$$\frac{\Delta\nu(t)}{\nu(t)} \equiv \frac{\nu_e(t) - \nu_g(t)}{\nu_g(t)} \tag{33}$$

between the transport collision frequencies of Cs atoms in the Ar buffer gas on the dimensionless velocity $t = v/v_T$ upon excitation of the D_1 transition of Cs atoms. Formula (24) shows that due to the factor $t\exp(-t^2)$ the main contribution to the drift-velocity integral $u(\Omega)$ is made by the particles with velocities $t \approx 1$. In the $t \approx 1$ region at $T = 300$ and 1500 K, the factor $\Delta\nu(t)/\nu(t)$ does not change its sign for the Cs–Ar system [curves (*1*) and (*3*) in Fig. 4]; therefore, one should observe at these temperatures the normal LID of Cs atoms, well described by the LID theory with velocity-independent transport collision frequencies. At $T = 970$ K the sign of the factor $\Delta\nu(t)/\nu(t)$ changes in the $t \approx 1$ region [curve (*2*) in Fig. 4] and thus in the vicinity of $T \approx 970$ K there must arise the anomalous LID of Cs atoms in the Ar buffer gas.

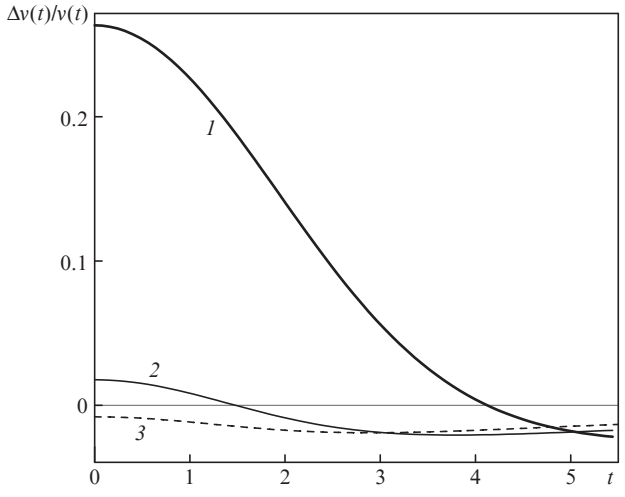

Figure 4. Dependences of the relative difference between the transport collision frequencies $\Delta\nu(t)/\nu(t)$ of the dimensionless velocity $t = v/v_T$ for the Cs–Ar system in the case of excitation of the D_1 transition of Cs atoms at $T =$ (*1*) 300, (*2*) 970 and (*3*) 1500 K.

In the numerical calculations, we assume that the spectrum of broadband radiation has a Gaussian shape:

$$F(\omega) = \frac{1}{\sqrt{\pi}\,\Delta\omega}\exp\left[-\left(\frac{\omega - \omega_b}{\Delta\omega}\right)^2\right], \tag{34}$$

where ω_b is the centre frequency of broadband radiation, and $\Delta\omega$ is the half-width (at 1/e level) of its spectrum. The value of $\Delta\omega$ is taken several greater than the Doppler width of the absorption line; in the calculations we used $\Delta\omega/2\pi = 3000$ MHz [$\Delta\omega/(2\pi c) = 0.1$ cm^{-1}]. With this value of $\Delta\omega$ the linewidth of broadband radiation is several times smaller than the frequency spacing between the HFS levels of the ground state and several times greater than the frequency spacing between the HFS levels of the excited state. The centre frequency ω_b is chosen such that broadband and monochromatic radiations affect different HFS levels of the ground state. Formally, this is reflected in the fact that in the case of the negative (positive) frequency detuning Ω of monochromatic radiation, the centre frequency ω_b of broadband radiation is equal to the frequency between the 'middle' of the HFS of the excited state and the HFS sublevel n (m) of the ground state:

$$\omega_b = \begin{cases} \omega_0 + \omega_{mn}/2, \text{ if } \Omega < 0, \\ \omega_0 - \omega_{mn}/2, \text{ if } \Omega > 0, \end{cases} \tag{35}$$

where ω_{mn} is the frequency spacing between the HFS levels of the ground state. As noted above, broadband radiation itself causes no LID effect, but provides its multiple enhancement due to the fact that it considerably reduces pumping of the atoms with one hyperfine component of the ground state to the other. With regard to the mutual direction of propagation of monochromatic and broadband radiations we assume that the waves can be copropagating (we will also use the notation $\boldsymbol{k}_b\uparrow\uparrow\boldsymbol{k}$) or counterpropagating ($\boldsymbol{k}_b\uparrow\downarrow\boldsymbol{k}$).

Figure 5 shows the results of the numerical calculations [based on formulas (22)–(26)] of the LID velocity projection to the direction of monochromatic radiation $u_L \equiv \boldsymbol{k}\boldsymbol{u}_L/k$ as a function of the frequency detuning Ω (27) for Cs atoms in the Ar buffer gas in the case of excitation of the D_1 transition of Cs atoms. The calculations were performed using velocity-dependent collision frequencies $\nu_k(v)$ (15) (solid curves) and velocity-independent collision frequencies [dashed curves; in the formulas for the drift velocity we used ν_k^{tr} (20) instead of $\nu_k(v)$ (15)]. All the calculations were performed at a buffer gas pressure of $p_{buf} = 10$ Torr. The LID velocity is virtually independent of the direction of propagation of broadband radiation: the dependences $u_L(\Omega)$ for the cases of copropagating and counterpropagating waves do not differ in the scales of the figure.

One can see from Fig. 5 that the velocity dependence of the collision frequencies can greatly change the shape of the LID line (compared with the results of calculations with constant collision frequencies), up to the appearance of additional zeros in the $u_L(\Omega)$ dependence. For Cs atoms the drift velocity as a function of the radiation frequency can have eleven zeros (Fig. 5b) instead of seven, as would be in the case of the normal LID (dashed curves in Fig. 5). The numerical calculations show that the anomalous LID of Cs atoms in the Ar buffer gas arises upon excitation of the D_1 line of caesium atoms in the temperature range 850 K $< T <$ 1150 K. Thus, in this temperature range it is necessary to take into account the velocity dependence of the collision frequencies, $\nu_k(v)$, in the calculation of the drift velocity (24). At lower, or vice versa, higher temperatures the velocity dependence of the collision frequencies in equation (24) has little effect on the shape of the LID line. In these temperature ranges, the drift velocity (24) can be calculated with good accuracy by using velocity-independent collision frequencies ν_k^{tr} (20) (Fig. 5a). Comparison of Figs 5a and 5b clearly shows that in the case of the anoma-

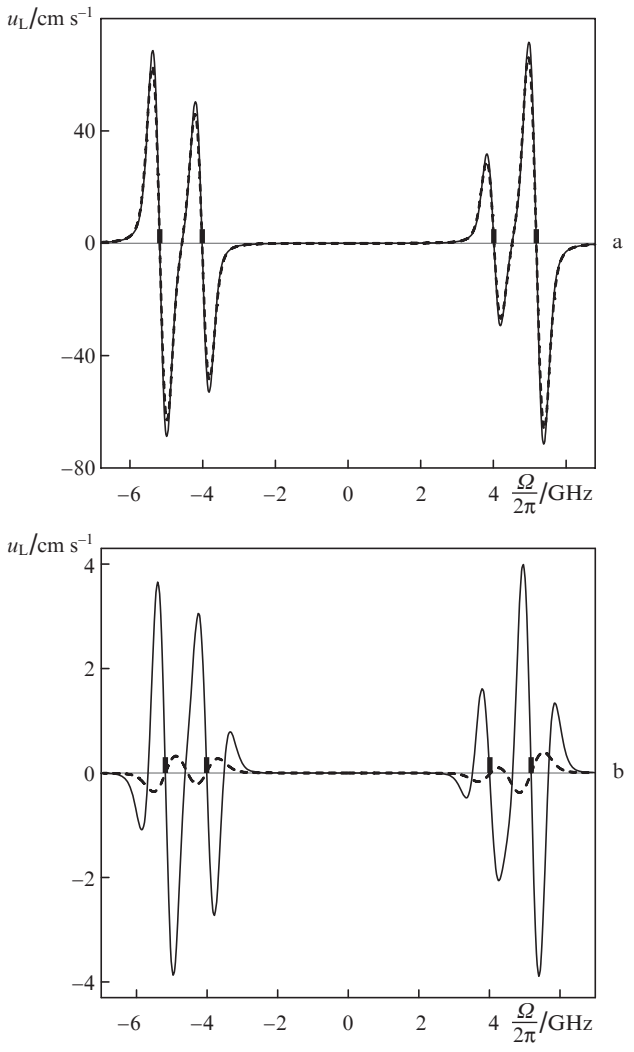

Figure 5. Dependences of the LID velocity projection to the direction of monochromatic radiation $u_L \equiv \boldsymbol{k}\boldsymbol{u}_L/k$ on the frequency detuning $\Omega = \omega - \omega_0$ of monochromatic radiation for Cs atoms in the Ar buffer gas in the case of excitation of the D_1 transition of Cs atoms at $p_{buf} = 10$ Torr, $I_m = 0.1$ W cm^{-2}, $I_b = 1$ W cm^{-2}, $\Delta\omega/(2\pi c) = 0.1$ cm^{-1}, T = (a) 300 and (b) 970 K. The dashed curves show the calculations without the velocity dependence of the transport collision frequencies [with the replacement $\nu_k(t) \to \nu_k^{tr}$]. The vertical lines indicate the frequencies that are resonant with the frequencies of the transitions m – 1, 2 and n – 1, 2.

lous LID of Cs atoms in the Ar buffer gas, the drift velocity decreases, as compared with the case of the normal LID, by approximately 20 times.

It is well known that the frequency dependence of the LID velocity is closely related with the absorption spectrum of monochromatic radiation. For example, in the simplest case of two-level particles and at constant collision frequencies, the frequency dependence of the drift velocity $u_L(\Omega)$ has the form of the first derivative of the absorption line. Figure 6 shows the results of the numerical calculations [by formulas (30) and (31)] of the probabilities of monochromatic radiation absorption. When using only a single travelling monochromatic wave, the effect of the optical pumping leads to the formation of a smooth single absorption line located between the resonant frequencies of the transitions from the HFS components [curve (*1*) in Fig. 6]. In a situation when the optical pumping is negligible (in the presence of broadband radiation), the absorption line of monochromatic radiation experiences significant changes: it is determined by a combination of individual lines corresponding to intra-atomic transitions [curve (*2*) in Fig. 6]. Such a transformation of the absorption spectrum of monochromatic radiation means that broadband radiation still has a significant effect on the shape of the LID line, though it does not result in the occurrence of the LID due to the velocity-nonselective interaction with the atoms. One can see from Fig. 6 that broadband radiation increases the probability of monochromatic radiation absorption by three orders of magnitude. Thus, when use is made of broadband radiation, the LID velocity increases by three orders of magnitude.

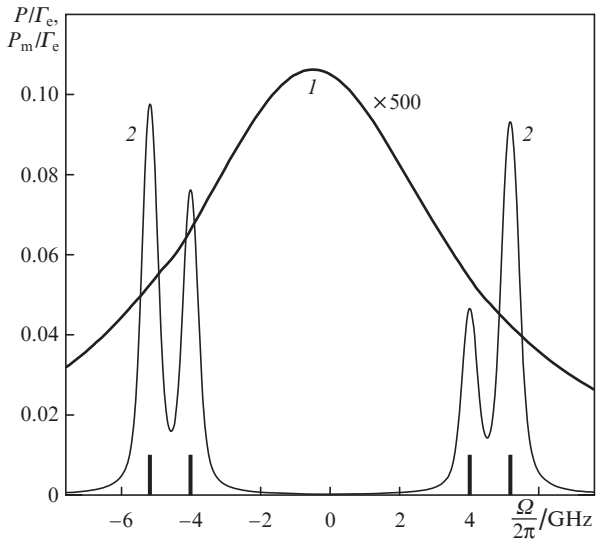

Figure 6. Probabilities of absorption of monochromatic radiation for Cs atoms in the Ar buffer gas for the D_1 line of Cs atoms at $T = 300$ K, $p_{buf} = 10$ Torr, $I_m = 0.1$ W cm^{-2}, $I_b = 1$ W cm^{-2}, $\Delta\omega/(2\pi c) = 0.1$ cm^{-1}: (*1*) probability P of absorption of monochromatic radiation (31) in the absence of broadband radiation (at $I_b = 0$) and (*2*) probability P_m of absorption of monochromatic radiation (30) in the presence of broadband radiation. The vertical lines indicate the frequencies that are resonant with the frequencies of the transitions m – 1, 2 and n – 1, 2.

Figure 7 shows the results of the numerical calculations [by formulas (29) and (30)] of the light-pressure-induced drift velocity projection to the direction of monochromatic radiation $u_R \equiv \boldsymbol{k}\boldsymbol{u}_R/k$ (calculations were performed with the same parameters as for Fig. 5a). As can be seen from Fig. 7, the drift velocity u_R strongly depends on the direction of propagation of monochromatic and broadband radiations: for counterpropagating waves it is eight times less than that for copropagating waves. Comparison of Figs 5 and 7 shows that in the case of counterpropagating waves, under the action of light pressure the maximum LID velocity exceeds the maximum drift velocity by 6000 and 330 times, respectively, for the cases of the normal (Fig. 5a) and anomalous (Fig. 5b) LIDs. On the basis of this fact, we have neglected the effect of light pressure in the calculations of the anomalous LID of caesium atoms.

Consider the LID of Cs atoms in the binary buffer mixtures of inert gases upon excitation of the D_1 transition of Cs atoms. In this case, as noted above, the anomalous LID of Cs atoms is possible at almost any temperature set by the experimenter if the fraction of the buffer gas in the binary buffer mixture is chosen appropriately. For definiteness, we

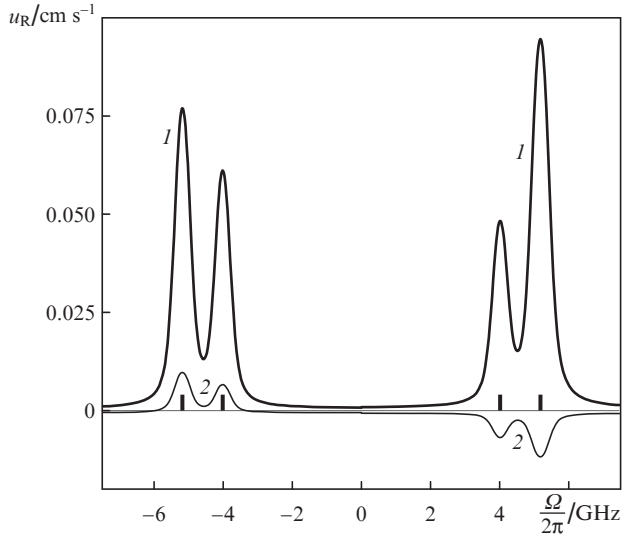

Figure 7. Dependences of the light-pressure-induced drift velocity projection to the direction of monochromatic radiation $u_R \equiv \boldsymbol{k}u_R/k$ on the frequency detuning Ω of radiation for Cs atoms in the Ar buffer gas in the case of excitation of the D_1 transition of Cs atoms at $p_{buf} = 10$ Torr, $T = 300$ K, $I_m = 0.1$ W cm^{-2}, $I_b = 1$ W cm^{-2}, $\Delta\omega/(2\pi c) = 0.1$ cm^{-1} for (*1*) $\boldsymbol{k}_b \uparrow\uparrow \boldsymbol{k}$ and (*2*) $\boldsymbol{k}_b \uparrow\downarrow \boldsymbol{k}$. The vertical lines indicate the frequencies that are resonant with the frequencies of the transitions m – 1, 2 and n – 1, 2.

will use $T = 300$ and 500 K. Figure 8 illustrates the occurrence of the anomalous LID of caesium atoms upon excitation of the D_1 transition of Cs atoms in the buffer gas mixture of Ne, He or Kr with any other gases, Ar or Xe, at various fractions of helium ξ_{He}, neon ξ_{Ne} and krypton ξ_{Kr} in these mixtures:

$$\xi_{Ne,He,Kr} = \frac{N_{Ne,He,Kr}}{N_b}, \quad N_b = N_{Ne,He,Kr} + N_X, \tag{36}$$

where $N_{Ne,He,Kr}$ is the concentration of neon (N_{Ne}), helium (N_{He}) or krypton (N_{Kr}); N_X is the concentration of other inert buffer gas (Ar or Xe); and N_b is the total concentration of the buffer gas. Note that the calculations of the drift velocity by the formulas for the normal LID [without the velocity dependence of the transport collision frequencies, i.e., with the replacement $\nu_k(t) \to \nu_k^{tr}$] at different (indicated in Fig. 8) fractions of helium, neon and krypton in the binary buffer mixture yield $u_L(\Omega) = 0$. Numerical analysis shows that at $T =$ 300 K, the anomalous LID of Cs atoms can be observed in the following ranges of the neon and helium fractions in the buffer mixture: $0.36 \lesssim \xi_{Ne} \lesssim 0.50$ for the Ne–Ar mixture; $0.920 \lesssim \xi_{He} \lesssim 0.945$ for the He–Ar mixture; $0.40 \lesssim \xi_{Ne} \lesssim 0.55$ for the Ne–Xe mixture; and $0.90 \lesssim \xi_{He} \lesssim 0.96$ for He–Xe the mixture. At $T = 500$ K the anomalous LID of Cs atoms can be observed in the range of krypton fractions, $0.37 \lesssim \xi_{Kr} \lesssim 0.67$, in the Kr–Ar mixture and, $0.67 \lesssim \xi_{Kr} \lesssim 0.85$, in the Kr–Xe mixture. The line shape of the anomalous LID is very sensitive to changes in the concentration of the components of the buffer mixture of the two gases.

Consider now the LID of Cs atoms in the case of excitation of the D_2 transition. Figure 9 shows the results of calculations of the LID velocity of Cs atoms in the Kr buffer gas. The calculations show that the anomalous LID of Cs atoms in the Kr buffer gas upon excitation of the D_2 line of caesium atoms occurs in the temperature range $800 \text{ K} < T < 1350$ K (Fig. 9b). Outside this range, the LID line shape corresponds to the normal LID and the drift velocity can be calculated by

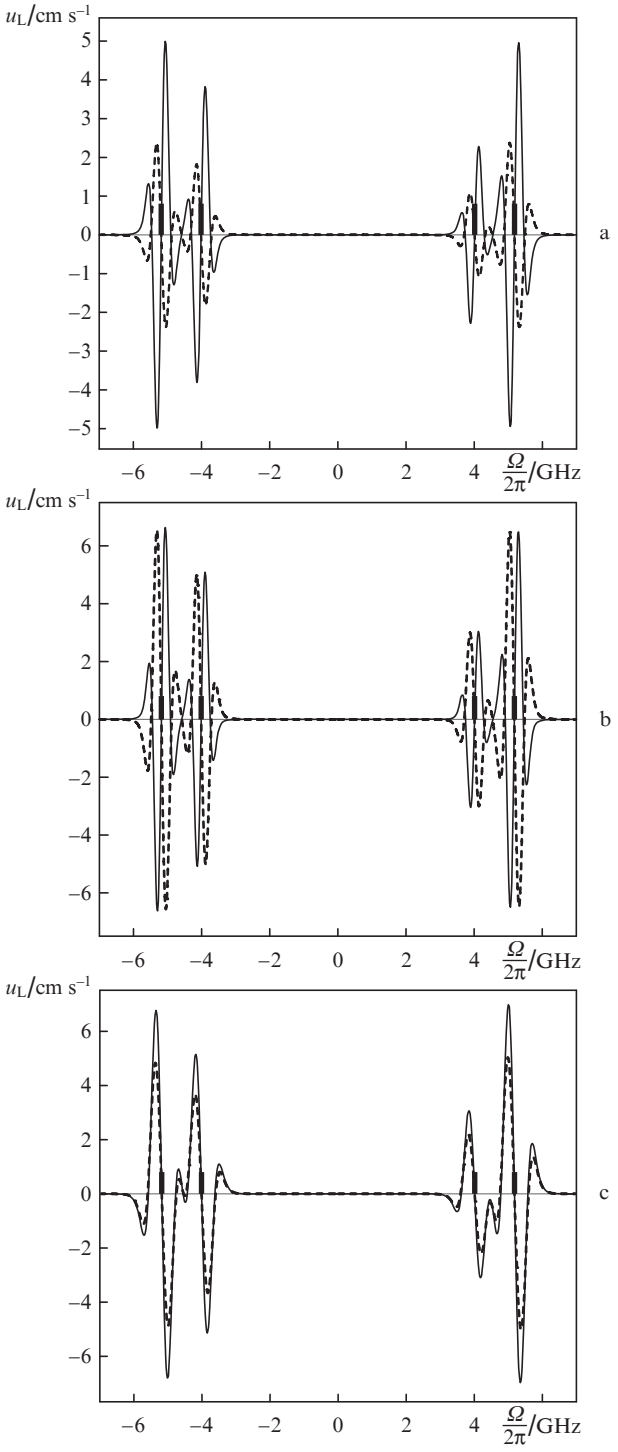

Figure 8. Dependences of the LID velocity projection to the direction of monochromatic radiation $u_L \equiv \boldsymbol{k}u_L/k$ on the frequency detuning Ω of monochromatic radiation for Cs atoms in the binary buffer mixtures in the case of excitation of the D_1 transition of Cs atoms at $p_{buf} = 10$ Torr, $I_m = 0.1$ W cm^{-2}, $I_b = 1$ W cm^{-2}, $\Delta\omega/(2\pi c) = 0.1$ cm^{-1}, $T =$ (a, b) 300 and (c) 500 K. The mixtures used are (a) Cs–(He–Xe) with $\xi_{He} = 0.945$ (solid line) and Cs–(He–Ar) with $\xi_{He} = 0.935$ (dashed line), (b) Cs–(Ne–Xe) with $\xi_{Ne} = 0.486$ (solid line) and Cs–(Ne–Ar) with $\xi_{Ne} = 0.442$ (dashed line) and (c) Cs–(Kr–Ar) with $\xi_{Kr} = 0.482$ (solid line) and Cs–(Kr–Xe) with $\xi_{Kr} = 0.750$ (dashed curve). The vertical lines indicate the frequencies that are resonant with the frequencies of the transitions m – 1, 2 and n – 1, 2. Calculations of the drift velocity, without the allowance for the velocity dependences of the transport collision frequencies (with the replacement $\nu_k(t) \to \nu_k^{tr}$], at the specified fractions of helium, neon and krypton in the binary buffer mixtures yield $u_L = 0$.

using the velocity-independent collision frequencies (Fig. 9a). Comparison of Figs 9a and 9b shows that in the case of the anomalous LID of Cs atoms in the Kr buffer gas, the drift velocity decreases by about eight times as compared with the case of the normal LID. The drift velocity dependences $u_L(\Omega)$ have a simpler form (fewer oscillations) compared with the case of the excitation on the D_1 line. This is due to the fact that the hyperfine splitting of the $6^2P_{3/2}$ level is comparable to the Doppler width or less than it (at room temperature the Doppler linewidth for caesium is $kv_T/2\pi$ = 230 MHz), and therefore the absorption line of monochromatic radiation is no longer a combination of separate lines corresponding to intra-atomic transitions, as in the case of excitation on the D_1 line.

The calculations show that when the D_2 line of caesium atoms is excited in the Ar buffer gas, the anomalous LIDs arises in the temperature range 800 K < T < 1250 K. At $T \approx$ 1030 K the line shape of the anomalous LID is the same as in Fig. 9b. At the same time, the drift velocities are about two times less than those shown in Fig. 9b.

When the D_2 line of Cs atoms is excited in the He buffer gas, the anomalous LID arises in the vicinity of $T \approx$ 325 K. However, the maximum value of the drift velocity in this case is too small – about 100 times less than that shown in Fig. 9b.

Figure 10 illustrates the occurrence of the anomalous LID of Cs atoms upon excitation of the D_2 transition of Cs atoms in the binary buffer mixture He–Kr with the helium fraction of ξ_{He} = 0.974 at T = 600 K. At the given temperature, the anomalous LID can be observed only in a narrow range of helium fractions in the buffer mixture: $0.960 \lesssim \xi_{He} \lesssim 0.985$.

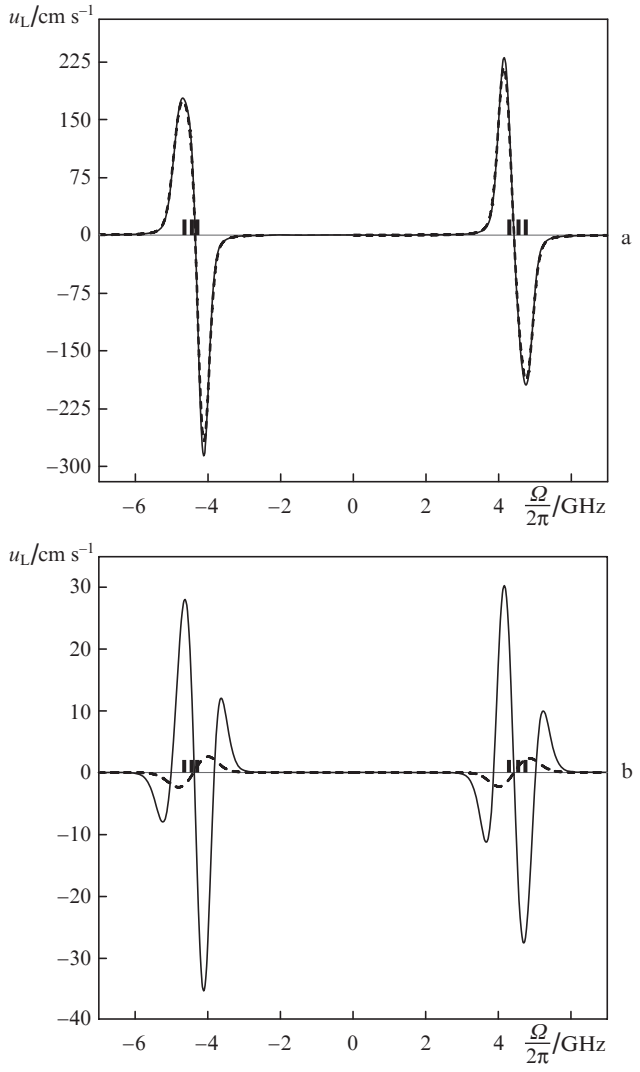

Figure 9. Dependences of the LID velocity projection to the direction of monochromatic radiation $u_L \equiv \boldsymbol{k}\boldsymbol{u}_L/k$ on the frequency detuning Ω of monochromatic radiation for Cs atoms in the Kr buffer gas in the case of excitation of the D_2 transition of Cs atoms at p_{buf} = 10 Torr, I_m = 0.1 W cm^{-2}, I_b = 1 W cm^{-2}, $\Delta\omega/(2\pi c)$ = 0.1 cm^{-1}, T = (a) 300 and (b) 1120 K. The dashed curves show the calculations without the allowance for the velocity dependence of the transport collision frequencies (with the replacement $\nu_k(t) \to \nu_k^{[r]}$). The vertical lines indicate the frequencies that are resonant with the frequencies of the transitions m – 1, 2 and n – 1, 2.

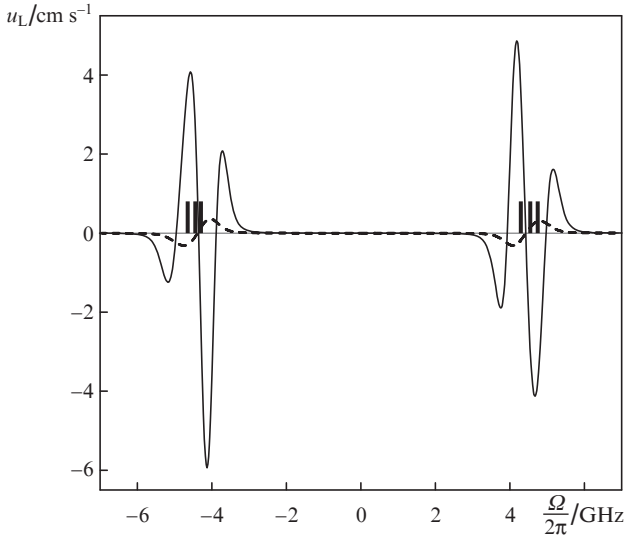

Figure 10. Dependences of the LID velocity projection to the direction of monochromatic radiation $u_L \equiv \boldsymbol{k}\boldsymbol{u}_L/k$ on the frequency detuning Ω of monochromatic radiation for Cs atoms in the He–Kr binary buffer mixture in the case of excitation of the D_2 transition of Cs atoms at T = 600 K, ξ_{He} = 0.974, p_{buf} = 10 Torr, I_m = 0.1 W cm^{-2}, I_b = 1 W cm^{-2}, $\Delta\omega/(2\pi c)$ = 0.1 cm^{-1}. The dashed curves show the calculations without the allowance for the velocity dependence of the transport collision frequencies [with the replacement $\nu_k(t) \to \nu_k^{[r]}$]. The vertical lines indicate the frequencies that are resonant with the frequencies of the transitions m – 1, 2 and n – 1, 2.

The numerical analysis shows that at T = 600 K the anomalous LID of Cs atoms can be observed upon excitation of the D_2 transition of Cs atoms in the following buffer mixtures: in the He–Ar mixture at $\xi_{He} \approx 0.935$, in the He–Xe mixture at $\xi_{He} \approx 0.991$ and in the He–Ne mixture at $\xi_{He} \approx 0.963$. At the given temperature the anomalous LID can be observed only in a narrow range of $\Delta\xi_{He} \approx 0.02$ in the buffer mixtures.

4. Conclusions

Using the known interatomic interaction potentials we have investigated the anomalous LID of caesium atoms upon excitation of the D_1 and D_2 line of Cs atoms in an inert buffer gas or binary buffer mixture of two different inert gases. We have predicted the anomalous frequency dependence of the drift velocity of caesium atoms in the Ar buffer gas in the temperature range 850 K < T < 1150 K upon excitation of the D_1 line of Cs atoms and in Ar and Kr buffer gases in the temperature

ranges 800 K < T < 1250 K and 800 K < T < 1350 K, respectively, upon excitation of the D_2 line of Cs atoms. We have found that in the binary buffer mixtures of the inert gases the anomalous LID of caesium atoms can be observed at almost any (including ambient) temperature, depending on the content of the buffer gases in the mixtures.

The results obtained show that even a small difference in the interatomic interaction potentials of resonant and buffer particles strongly manifests itself in the frequency dependence of the drift velocity in the region of the anomalous LID. Experimental study of the anomalous LID of caesium atoms will allow one to test the subtle details of the interatomic interaction potentials.

Acknowledgements. The authors thank J. Pascale for kindly providing detailed tabular data on the interaction potentials of alkali metal atoms with the atoms of the inert gases.

This work was supported by the Russian Foundation for Basic Research (Grant No. 13-02-00075-a), the DPS RAS programme 'Fundamental Optical Spectroscopy and Its Applications' (Project No. III.9.1) and the RF President's Grants Council (Support to Leading Scientific Schools Programme, Grant No. NSh-2979.2012.2).

References

1. Gel'mukhanov F.Kh., Shalagin A.M. *Pis'ma Zh. Eksp. Teor. Fiz.*, **29**, 773 (1979).
2. Antsygin V.D., Atutov S.N., Gel'mukhanov F.Kh., Telegin G.G., Shalagin A.M. *Zh. Eksp. Teor. Fiz*., **30**, 262 (1979).
3. Rautian S.G., Shalagin A.M. *Kinetic Problems of Nonlineyar Spectroscopy* (Amsterdam–New York: Elsevier Science Publ. Comp., 1991).
4. Nienhuis G. *Phys. Rep*., **138**, 151 (1986).
5. Werij H.G.C., Woerdman J.P. *Phys. Rep*., **169**, 145 (1988).
6. Chapovsky P.L. *Izv. Akad. Nauk SSSR, Ser. Fiz*., **53**, 1069 (1989).
7. Eliel E.R. *Adv. At. Mol. Opt. Phys*., **30**, 199 (1992).
8. Nagels B., Chapovsky P.L., Hermans L.J.F., van der Meer G.J., Shalagin A.M. *Phys. Rev. A*, **53**, 4305 (1996).
9. Van Duijn E.J., Nokhai R., Hermans L.J.F. *J. Chem. Phys.*, **105**, 6375 (1996).
10. Popov A.K., Shalagin A.M., Shalaev V.M., Yakhnin V.Z. *Zh. Eksp. Teor. Fiz*., **80**, 2175 (1981).
11. Atutov S.N., Ermolaev I.M., Shalagin A.M. *Zh. Eksp. Teor. Fiz*., **92**, 1215 (1987).
12. Van der Meer G.J., Smeets J., Pod'yachev S.P., Hermans L.J.F. *Phys. Rev. A*, **45**, R1303 (1992).
13. Van der Meer G.J., Broers B., Chapovsky P.L., Hermans L.J.F. *J. Phys. B*, **25**, 5359 (1992).
14. Chapovsky P.L., van der Meer G.J., Smeets J., Hermans L.J.F. *Phys. Rev. A*, **45**, 8011 (1992).
15. Van der Meer G.J., Smeets J., Eliel E.R., Chapovsky P.L., Hermans L.J.F. *Phys. Rev. A*, **47**, 529 (1993).
16. Van Duijn E.J., Bloemink H.I., Eliel E.R., Hermans L.J.F. *Phys. Lett. A*, **184**, 93 (1993).
17. Kuščer I., Hermans L.J.F., Chapovsky P.L., Beenakker J.J.M., van der Meer G.J. *J. Phys. B*, **26**, 2837 (1993).
18. Yahyaei-Moayyed F., Streater A.D. *Phys. Rev. A*, **53**, 4331 (1996).
19. Gel'mukhanov F.Kh., Parkhomenko A.I. *Phys. Lett. A*, **162**, 45 (1992).
20. Gel'mukhanov F.Kh., Parkhomenko A.I. *Zh. Eksp. Teor. Fiz.*, **102**, 424 (1992).
21. Gel'mukhanov F.Kh., Kharlamov G.V., Rautian S.G. *Opt. Commun*., **94**, 521 (1992).
22. Gel'mukhanov F.Kh., Parkhomenko A.I. *J. Phys. B*, **28**, 33 (1995).
23. Gel'mukhanov F.Kh., Parkhomenko A.I., Privalov T.I., Shalagin A.M. *J. Phys. B*, **30**, 1819 (1997).
24. Parkhomenko A.I. *Zh. Eksp. Teor. Fiz*., **115**, 1664 (1999).
25. Parkhomenko A.I. *Zh. Eksp. Teor. Fiz*., **116**, 1587 (1999).
26. Parkhomenko A.I., Shalagin A.M. *Zh. Eksp. Teor. Fiz*., **145**, 223 (2014).
27. Pascale J., Vandeplanque J. *J. Chem. Phys*., **60**, 2278 (1974).
28. Happer W. *Rev. Mod. Phys*., **44**, 169 (1972).
29. Aleksandrov E.B., Khvostenko G.I., Chaika M.P. *Interferentsiya atomnykh sostoyanii* (Interference of Atomic States) (Moscow: Nauka, 1991).
30. Sobel'man I.I. *Introduction to The Theory of Atomic Spectra* (London, Pergamon, 1972; Moscow: Nauka, 1977).
31. Varshalovich D.A., Moskalev A.N., Khersonskii V.K. *Kvantovaya teoriya uglovogo momenta* (Quantum Theory of Angular Momentum) (Leningrad: Nauka, 1975).
32. Il'ichev L.V., Parkhomenko A.I. *Zh. Eksp. Teor. Fiz*., **112**, 856 (1997).
33. Gel'mukhanov F.Kh., Il'ichov L.V., Shalagin A.M. *Physica A*, **137**, 502 (1986).
34. Hamel W.A., Haverkort J.E.M., Werij H.G.C., Woerdman J.P. *J. Phys. B*, **19**, 4127 (1986).
35. NIST Atomic Spectra Database. http://www.nist.gov/pml/data/asd.cfm.
36. Parkhomenko A.I., Shalagin A.M. *Kvantovaya Elektron*., **43**, 162 (2013) [*Quantum Electron*., **43**, 162 (2013)].
37. Allard N., Kielkopf J. *Rev. Mod. Phys*., **54**, 1103 (1982).